第 30 屆海洋工程研討會論文集 國立交通大學 2008 年 11 月
Proceeding of the 30th Ocean Engineering Conference in Taiwan
National Chiao Tung University, November 2008

Method of Fundamental Solutions for Acoustic Wave Propagation in Shallow Water Region

Ching-Sen Wu[1] Der-Liang Young[2]

[1]Graduate Student, Department of Civil Engineering and Hydrotech Research Institute, National Taiwan University
[2]Professor, Department of Civil Engineering and Hydrotech Research Institute, National Taiwan University

ABSTRACT

An approach combining the method of fundamental solutions (MFS) in conjunction with the normal modes technique (NMT) is proposed to simulate the acoustic wave propagation over the shallow water region. It is assumed that the sound-speed is the isovelocity profile, the free surface is quiescent and the topography of seabed is rugged. The considered model, ranging from smooth to abrupt variation, is descritized into simple rectangular geometry and cosine bell deformation at the bottom in terms of the irregular topography. Mathematical formulations of the eigenfunction expansion, in point of NMT, are implemented clearly to describe the radiation conditions on the open boundaries. Effects of node resolution and small aspect ratios over the computational domain are discussed. Accuracy of the results by the proposed approach is assessed and verified by comparison with analytic solution and the boundary element method (BEM).

Keywords: method of fundamental solutions; normal modes technique; acoustic wave propagation; irregular seabed topography; radiation condition

基本解法於淺水區域之聲波傳遞分析

吳清森 楊德良

摘要

本文藉由結合基本解法與正交模態法來模擬淺水區域中的聲波傳遞現象。文中假設水中的聲速皆爲等速，自由液面則爲靜止的狀態以及海床爲崎嶇的地形。不規則的海床地形則分別以簡易的長方形幾何以及如鐘型般的餘弦變形幾何模擬之。正交模態技巧則利用數學中特徵函數展開法來描述遠域輻射邊界條件。於計算過程中，點數的選取及相異尺寸大小的幾何圖形皆於文中探討；此外，使用基本解法結合正交模態法所得到的數值解與解析解以及邊界元素法做精確度上的比較。

關鍵詞:基本解法、正交模態技巧、聲波傳遞、不規則的海床地形、輻射條件

1. Introduction

Classical numerical methods are usually divided into two main categories: the boundary-type method and the domain-type method. The classical numerical methods, requiring domain or boundary discretization, have not widely used to compute the propagation of sound because of the high computation cost entailed. For this reason, to overcome the above mentioned drawbacks of classical numerical schemes and to develop numerical methods which require neither domain nor boundary discretazation, it is the purpose to introduce the MFS in this paper to analyze the shallow water problem with source excitation which can avoid the time-consuming problem originated in mesh generation for rugged topographies. However,

the mentioned MFS, originally introduced by Kupradze in Russian in 1964, was strongly recommended by Golberg *et al.*. The numerical implementation of the MFS is very simple since there is no need to solve integral equations, relating a set of virtual sources placed over a surface outside the domain in order to avoid the integration of singularities that arise in other methods.

The principal characteristic of shallow water propagation is that the sound speed profile is downward refracting or nearly constant over depth. Most common techniques used to analyze the underwater acoustic wave propagation can be classified as three schemes. They are ray-theory (Arnold and Felsen, 1983), normal mode solutions with adiabatic approximation or mode coupling (Evans, 1983) and parabolic equation models have been utilized successfully in shallow water environment as indicated by Jensen *et al.* in 1984. In 1998, Grilli *et al.* firstly proposed a hybrid numerical model subject to the integration techniques which are implemented in BEM for calculating singular and quasi-singular integrals. Later, in 2000, Santiago and Wrobel proposed the boundary element formulation in conjunction with the sub-region techniques for 2D acoustic wave propagation in shallow water. Due to the comparative merits of each classical numerical scheme that we mentioned before, in the present article, the MFS is employed accurately to study the two-dimensional acoustic wave propagation in shallow water with arbitrary geometry at the bottom under the excitation by sources.

2. Problem Statements and Mathematical Formulations

Consider the wave propagation of underwater acoustic problem over an irregular seabed Ω as shown in Fig.1. The model is divided into two types of topographies, include rectangular geometry and cosine-bell shape in our analyzed process in which the free surface is atmospheric pressure and the seabed is rigid, hence, no-flow condition applies. The problem of interest is a two-dimensional problem in the vertical plane (x, z), with constant sound velocity c.

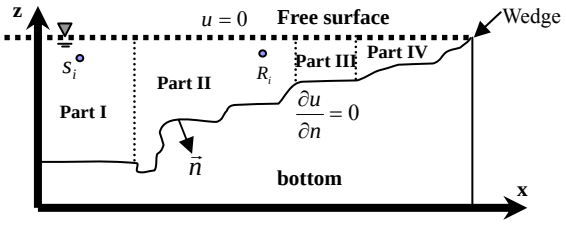

Fig. 1 The sketch of regions dividing a typical shallow water section.

Assuming that the medium of ideal fluid in the absence of perturbations is quiescent under consideration, we have the linear wave equation as follows:

Continuity equation:

$$\frac{\partial \rho}{\partial t} = -\rho \nabla \cdot \vec{u} \cdot \tag{1}$$

Momentum equation:

$$\rho \frac{\partial \vec{u}}{\partial t} = -\nabla p \cdot \tag{2}$$

State equation:

$$p = \rho\, c^2 \cdot \tag{3}$$

The complex potential can be defined as $U(x,z,t) = \phi(x,z)e^{-iwt}$ with the velocity $\vec{u} = \nabla U$, in which ω is the angular frequency of acoustic wave and ϕ is the potential amplitude. After combing Eqs.(1)-(3) with the acoustic disturbance is time-harmonic, the governing equation reduces to Helmholtz equation in domain Ω,

$$(\nabla^2 + k^2)\phi = -\sum_{i=1}^{N} \alpha_i \delta(x_{\alpha_i}, z_{\alpha_i}), \quad (x,z) \in \Omega, \tag{4}$$

where k is the wavenumber, α_i is the magnitude of point source located at $(x_{\alpha_i}, z_{\alpha_i})$, $\delta(\bullet)$ is the Dirac-delta function and N is the quantities of the point source. Three typical boundary conditions for boundary geometries are considered in the two-dimensional acoustic wave propagation problem. Due to the no-flow condition at the rigid seabed, we

have zero penetration velocity

$$\frac{\partial \phi(x)}{\partial n} = 0, \quad x \in B, \tag{5}$$

where n is the unit outward normal vector on the real boundary. At the free surface, we assume that the atmospheric pressure is equal to zero in all regions. In light of the ideal fluid theory, the relation between the velocity potential and pressure potential is simplified by the Bernoulli equation in the form of

$$p(x) = -i\omega\rho\phi(x), \quad x \in B. \tag{6}$$

In other words, the boundary condition is then given by $\phi(x) = 0, \quad x \in B$. In this present work, those boundary conditions are simulated by the normal modes technique (or called eigenfunction expansion scheme) and constructed by the contributions of the modes weighted in accordance to the source depth which are roughly akin to the modes of a vibrating string. Under the circumstances of the depth-dependent of normal modes, the potential normal gradient on the open boundaries is represented as follows:

$$\frac{\partial \phi(x,z)}{\partial n} = \sum_{m=1}^{M} \frac{-2i}{h} \frac{\sqrt{k^2 - k_m^2}}{k_m} \sin(k_m z)\left[1 - \cos(k_m H)\right] \tag{7}$$

where k_m is the vertical wave number with mth mode, H is the depth of considered shallow water and M is the number of modes that we choose. However, the number of modes that we employed is investigated to simulate the fictitious boundaries of infinite extent which have both propagating and evanescent components.

3. Numerical Method ─Method of Fundamental Solutions

MFS is a technique for the numerical solution of certain boundary value problems and it shares the same advantages as the BEM over domain discretization methods. The basic idea for the method of fundamental solutions, the free-space Green's function, is the approximate solution $u(x)$ is superimposed by the fundamental solutions of the governing equation, $U(x,s)$, expressed as a linear combination

$$u(x) = \sum_{j=1}^{N} c_j G(x, s_j), \quad s_j \in \Omega^e, \tag{8}$$

with the singularities s_j outside the domain of the problem. Where N is the number of source points in the MFS, c_j is the j^{th} unknown coefficient, *s* and *x* are the source point and collocation point, respectively, Ω^e is the complementary domain and $G(x,s)$ is the corresponding fundamental solution. The numerical scheme depends on the position of a fixed number of sources located outside the domain as depicted in Fig.2.

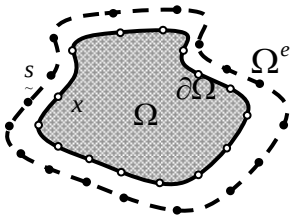

Fig.2 The node distributions for the boundary grid of the MFS. Real line is the virtual boundary of the domain; dotted line is the fictitious boundary.

To demonstrate the acoustic wave propagation problem by MFS, the fundamental solution and its normal derivative of 2D Helmholtz equation are respectively derived as

$$G(x,s) = \frac{-2i}{\pi} H_0^{(1)}(kr) = \frac{2}{\pi}\left[iJ_0(kr) + Y_0(kr)\right], \quad r \equiv \|x - s\|, \tag{9}$$

$$\frac{\partial G(x,s)}{\partial n} = k\left[\frac{iJ_1(kr) - Y_1(kr)}{r}\right] y_i \bar{n}_i. \tag{10}$$

where r is the distance between the source point s and boundary point x and y_i is the vector component denotes as $y_i = x_i - s_i, i = 1, 2.$

4. Numerical Examples and Discussions

In order to demonstrate the accuracy of the MFS, two benchmark numerical examples of a standard two-dimensional inhomogeneous Helmholtz equation

are considered. Simple rectangular geometry with small domain aspect ratios and cosine-bell shape on the bottom are employed in our numerical tests due to the variations of the topography close to shore. After that, the irregular topography of cosine-bell shape is considered. For simplicity, we assume that the strength of acoustic source is unit magnitude, allowing the sound waves whose velocity is taken as $c = 1500$ *m/s* under consideration. In light of these definitions, the error of the numerical solution for test case is measured by calculating the root mean square error (RMSE) between the MFS and the analytic solution.

4.1 Rectangular geometry

Consider the first test problem is given by specifying three rigid boundaries and a uniform potential on the fourth boundary as depicted in Fig.3 with the dimension $L \times H$. For simplicity, we assume that the dimensions of length and height are both equal to one.

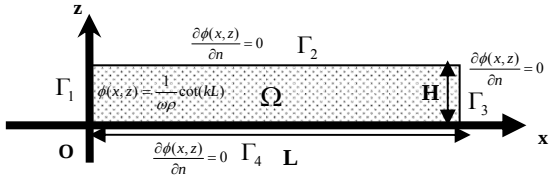

Fig. 3 Geometry for the rectangular domain.

Computations have been performed in the frequency domain in which the wavenumber k from 1.0 to 8.0 with an increment of $dk = 0.001$. Best distance between the virtual and physical boundary is set at 0.2. The closed-form analytic solution to this problem is easily to derive as follows:

$$\phi(x,z) = \frac{1}{\omega\rho}\left\{\sin(kx) + \frac{\cos(kx)}{\tan(kL)}\right\}, \tag{11}$$

RMSE for rectangular domain with velocity potential and its normal gradient are shown in Figs. 4 and 5. To compare the numerical results by the MFS with those by BEM (linear element with the Guassian points is $\mathrm{P} = 10$) in Ref. 5, the accuracy of the two referenced numerical methods are explicit to differentiate under the same wavenumbers, thus read, $k = 6.284, 6.478, 7.854$ for the velocity potential and $k = 6.283, 7.792$ for the normal gradient.

The wavenumber which the solution gives the least accuracy coincide with the resonant frequency and anti-resonant frequency, respectively. Note that the large errors when $k = 6.478$ in Fig. 4 are not identical to those when resonance and anti-resonance occur. Shapes of the wave propagation, when $k = 6.284, 6.478, 7.854$, along the x-axis are shown in Figs. 6(a)-(c), respectively. Convergence of RMSE in this case, $kH = 6.6$, by the proposed approach is discussed and compared with BEM in Fig. 7 with the variations of number of nodes per wavelength. It is obvious to investigate that the solution converges when the nodes increase. Moreover, as the domain aspect ratios decrease, from 0.5 to 0.1, with the length-dependent rectangular geometry are displayed in Fig.10, using $kH = 3.5$. Results of RMSE are shown in Fig. 8 for different number of points, from which we can see that they are not in direct proportion when the nodes increase.

4.2 Cosine-bell deformation at the seabed

Consider the second numerical test, ranging from smooth for the first case to abrupt variation, is the coastal area with a simple cosine-bell deformation at the seabed. The interested model is in a rectangular slab of size $[-200m, 200m]\times[0m, 200m]$ whose acoustic source is located at the position $(0m, 150m)$. However, the deformed cosine-bell at the seabed is described by the sinusoidal function as follows:

$$f(x) = 25\left\{1 + \cos\left[\pi x / 50\right]\right\}. \tag{12}$$

Nodes distributions for the collocation points and fictitious source points of the considered cosine-bell shape and its normal derivative are depicted in Fig. 9. Due to the limitation of computer's inherent precision, the shape of the virtual boundary may influence the numerical accuracy of the results by MFS. In this case,

the circular virtual boundary is adopted to simulate such an irregular geometry in which 72 source points are employed. The assessment of the effectiveness by MFS is also proved by Wang and Qin (2006). Note that the *m*th mode in Eq. (12) has m zeros. Computations have been performed in the frequency domain from 15*Hz* to 150 *Hz*, with an increment of 2.5 *Hz*. Amplitude of the velocity potential along the cosine-bell deformation is showed in Fig. 10 for four selected frequencies, they are 15*Hz*, 35*Hz*, 50*Hz* and 100*Hz*. Good agreements show that the study work in this case is reasonable.

5. Conclusions

A MFS algorithm using fundamental solutions subject to an inhomogeneous Helmholtz equation has been developed and validated for modeling the underwater acoustic wave propagation problem over the shallow water region. The additive scheme in this article, normal modes technique, is adopted to simulate the radiation condition along fictitious boundary of infinite extent. The series of mathematical simulation improves the speed of convergence dramatically in terms of normal modes. Two kinds of irregular topographies close to the shore are commonly discussed. Numerical results are clearly shown that the MFS, which is free of mesh generation, can achieve very good accuracy with relatively small number of fictitious sources outside the domain and interpolation points. Through this study, excellent agreements by comparison with the analytic and the BEM results indicate the effectiveness of the proposed approach for acoustic wave propagation problem.

6. Acknowledgement

Financial support from the National Science Council of Taiwan is gratefully acknowledged. It is granted to the National Taiwan University under Grant No. NSC-96-2221-E-002-116.

7. References

1. Arnold, J.M. and Felsen, L.B. (1983) “Rays and local modes in a wedge-shaped ocean,” *J. Acoust. Soc. Am.*, Vol.73, pp.1105-1119.

2. Chen, J.T., Wu, C.S., Lee, Y.T. and Chen, K.H. (2007) “On the equivalence of the Trefftz method and method of fundamental solutions for Laplace and biharmonic equations,” *Comp. Math. Appl.*, Vol.53, pp.851-879.

3. Evans, R.B. (1983) “A coupled mode solution for acoustic propagation in a waveguide with stepwise depth variations of a penetrable bottom,” *J. Acoust. Soc. Am.*, Vol.84, pp.188-195.

4. Golberg, M.A. (1995) “The method of fundamental solutions for Poisson’s equation,” *Engng. Ana. Bound. Elem.*, Vol. 16, pp. 205-213.

5. Grilli, S., Pedersen, T. and Stepanishen, P. (1998) “A hybrid boundary element for shallow water acoustic propagation over an irregular bottom,” *Engng. Ana. Bound. Elem.*, Vol. 21, No.2, pp. 131-145.

6. Jesen, F.B., Kuperman, W.A., Poter, M.B. and Schmidt H. (1994) “*Computational Ocean Acoustics*,” American Institute of Physics, Woodbury, New York.

7. Kupradze, V. D. (1964) **“**A method for the approximate solution of limiting problems in mathematical physics, “*Comp. Mat. Math. Phy.*, Vol.4, pp.199-205.

8. Santiago, J.A.F. and Wrobel, L.C. (2000) “A boundary element model for underwater acoustics in shallow water,” *Comp. Model. Engng. Sci.*, Vol.1, No.3, pp. 73-80.

9. Wang, H. and Qin, H.W. (2006) “A meshless method for generalized linear or nonlinear Poisson-type problems,” *Engng. Ana. Bound. Elem.*, Vol. 30, pp. 515-521.

10. Young, D.L., Chen, C.W., Fan, C.M. and Tsai, C.C. (2006) “The method of fundamental solutions with eigenfunction expansion method for nonhomogeneous diffusion equation,” *Num. Meth. Part. Diff. Equ.*, Vol. 22, No.5, pp.1173-1196.

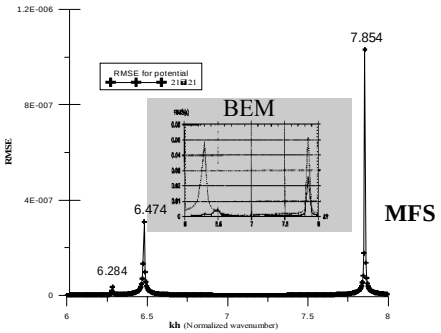

Fig. 4 RMSE for the velocity potential subject to the rectangular case using the MFS.

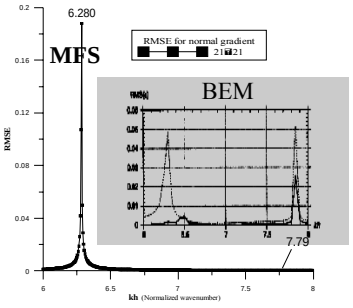

Fig. 5 RMSE for the potential normal gradient subject to the rectangular case using the MFS.

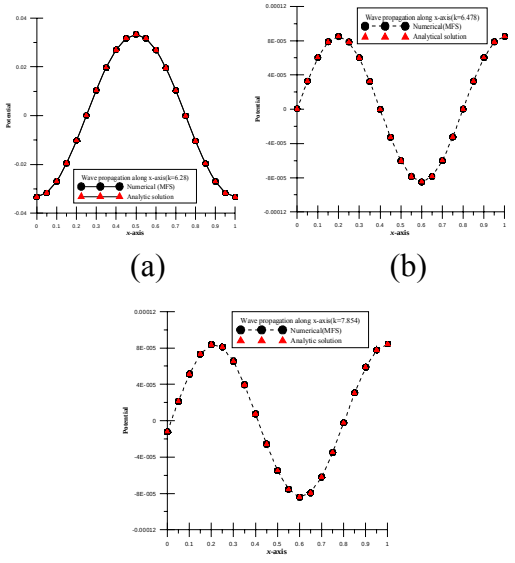

Fig. 6 Shape of the wave propagation with the wavenumber. (a) 6.284; (b) 6.478; (c) 7.854

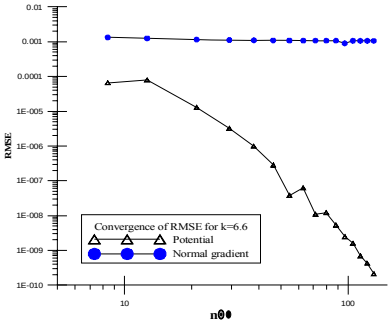

Fig. 7 Convergence of RMSE for rectangular domain

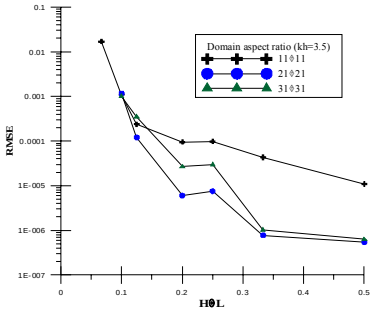

Fig. 8 Domain aspect ratios with different node distributions.

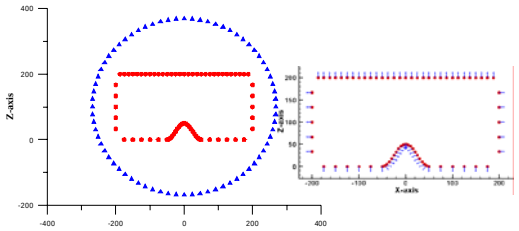

Fig. 9 Demonstrations of the collocation points and source points and its normal derivative.

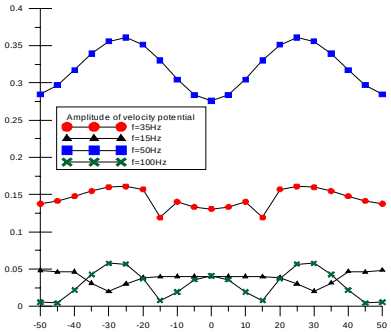

Fig. 10 Amplitude of the velocity potential along the cosine-bell deformation.